### Title
Atomic force microscopy investigation of Mason–Pfizer monkey virus and human immunodeficiency virus type 1 reassembled particles




### Journal
Virology, 360(2)

### ISSN
0042-6822



### Authors
Kuznetsov, Yu G
Ulbrich, P
Haubova, S
et al.



### Publication Date
2007-04-01

### DOI
10.1016/j.virol.2006.10.015

Available online at www.sciencedirect.com
ScienceDirect
Virology 360 (2007) 434–446
VIROLOGY
www.elsevier.com/locate/yviro

# Atomic force microscopy investigation of Mason–Pfizer monkey virus and human immunodeficiency virus type 1 reassembled particles

Yu. G. Kuznetsov [a], P. Ulbrich [b,c], S. Haubova [b], T. Ruml [b,d], A. McPherson [a,*]

[a] *Department of Molecular Biology and Biochemistry, University of California, Irvine, 560 SH, Irvine, CA 92697-3900, USA*
[b] *Institute of Chemical Technology, Technicka 5, 166 28 Prague 6, Czech Republic*
[c] *Institute of Molecular Genetics, Czech Academy of Sciences, 166 10 Prague, Czech Republic*
[d] *Institute of Organic Chemistry and Biochemistry, Czech Academy of Sciences, 166 10 Prague, Czech Republic*

Received 27 August 2006; returned to author for revision 18 September 2006; accepted 6 October 2006
Available online 22 November 2006

**Abstract**

Particles of ΔProCANC, a fusion of capsid (CA) and nucleocapsid (NC) protein of Mason–Pfizer monkey virus (M-PMV), which lacks the amino terminal proline, were reassembled *in vitro* and visualized by atomic force microscopy (AFM). The particles, of 83–84 nm diameter, exhibited ordered domains based on trigonal arrays of prominent rings with center to center distances of 8.7 nm. Imperfect closure of the lattice on the spherical surface was affected by formation of discontinuities. The lattice is consistent only with plane group p3 where one molecule is shared between contiguous rings. There are no pentameric clusters nor evidence that the particles are icosahedral. Tubular structures were also reassembled, *in vitro*, from two HIV fusion proteins, ΔProCANC and CANC. The tubes were uniform in diameter, 40 nm, but varied in length to a maximum of 600 nm. They exhibited left handed helical symmetry based on a p6 hexagonal net. The organization of HIV fusion proteins in the tubes is significantly different than for the protein units in the particles of M-PMV ΔProCANC.


*Keywords:* Retrovirus; Capsid; Architecture; Gag protein; Symmetry

## Introduction

Mason–Pfizer monkey virus (M-PMV) is a type D retrovirus which preassembles immature capsids in the cytoplasm prior to transport to the host cell membrane where they are released. Maturation then takes place. Bacteria expressing M-PMV Gag protein, and various truncated forms of Gag, produce spherical particles in inclusion bodies, and these exhibit features suggestive of icosahedral symmetry (Nermut et al., 2002). The particles, by electron microscopy, are indistinguishable from immature capsids made in mammalian cells. Protein extracted from the particles made in bacteria will reassemble *in vitro*, under specific conditions, to produce particles having the same appearance as the original (Klikova et al., 1995). Thus, it might reasonably be concluded that the *in vitro* reassembled particles are a good structural model for immature M-PMV capsids.

It has further been shown that the minimal protein construct that can produce reassembly products is a fusion of the capsid protein (CA) and the nucleocapsid protein (NC), termed CANC. That protein normally self assembles into two dimensional sheets in bacteria (Rumlova-Klikova et al., 2000). If, however, the amino terminal proline is deleted from the CA domain, then the ΔProCANC assembles into the spherical particles observed to be made in bacteria. The terminal proline residue, by virtue of its ability to hydrogen bond to aspartate 50, apparently exerts a profound influence on the overall assembly process (Rumlova-Klikova et al., 2000).

An earlier study by electron microscopy of reassembled products of Δp4Gag and ΔProCANC from M-PMV, including the spherical particles, was carried out using a variety of sample preparation and analysis techniques, including freeze fracture, negative staining and image processing (Nermut et al., 2002). That investigation showed the particles to have diameters ranging from 85 to 100 nm and to exhibit a hexagonal lattice of rings on their spherical surfaces. More recent work, again using electron microscopy (Ulbrich et al., 2006), reports an average

* Corresponding author.
*E-mail address:* amcphers@uci.edu (A. McPherson).

0042-6822/$ - see front matter © 2006 Elsevier Inc. All rights reserved.
doi:10.1016/j.virol.2006.10.015

diameter of 75 nm. The lattice suggested the possibility of icosahedral symmetry for the particles, though this could not be definitively demonstrated.

Three possible arrangements of protein molecules were considered as explanations for the observed surface lattice. Ultimately, one lattice, based on the sharing of a single protein molecule between adjacent rings of protein, was selected as the most probable. That lattice, however, was not the same as the lattice concluded to represent the surface structure of reassembled HIV-1 CA or Gag proteins in other, independent analyses (Ganser et al., 1999; Li et al., 2000; Nermut et al., 1998).

In contrast, the HIV-1 cores formed *in vitro* from purified CANC fusion protein were composed of helices of hexameric rings arrayed on conical hexagonal lattices (derived from plane group symmetry p6) which were thought to be closed by pentameric "defects" at the narrow and wide ends of the cones (Ganser et al., 1999). Unlike the M-PMV Δp4Gag and ΔProCANC, these particles did not share subunits between neighboring hexamers in their surface lattices. Similar organization was also described for His-tagged M-MuLV CA assembled on a lipid monolayer doped with nickel-chelating lipids (Ganser et al., 2003) and 2D crystals of RSV CA (Mayo et al., 2003). Barklis and collaborators have shown that 2D crystals of the same protein i.e. M-MuLV CA, can lead to different interpretations. One reconstruction shows a CA lattice exhibiting no symmetry (McDermott et al., 2000), in contrast to two others having hexagonal arrangements (Mayo et al., 2002, 2003). Thus, the question remained as to whether the reassembled M-PMV particles and reassembled HIV-1 products were constructed according to fundamentally different protein arrangements or whether some technical difference was responsible for the apparent inconsistency.

We undertook a further investigation of the spherical particles reassembled from M-PMV ΔProCANC using atomic force microscopy (AFM) in an attempt to resolve the question. The particles investigated by AFM were fully hydrated and were not stained or subjected to any other physical processes such as freezing. In addition, with AFM, we were able to visualize individual particles and were not dependent on the appearance or properties of populations. We also analyzed reassembly products, which were in most cases tubular assemblies, of HIV-1 fusion proteins. In particular, we addressed the questions of whether the reassembled ΔProCANC particles of M-PMV were indeed icosahedral, what was the fundamental symmetry of their surface lattice, what was the assembly unit of the lattice and what was the basis of the structural difference observed to exist between the M-PMV and HIV-1 reassembly products.

## Results

### *M-PMV ΔProCANC reassembled particles*

Particles of ΔProCANC protein, assembled *in vitro* in the presence of MS2 RNA under conditions previously described (Ulbrich et al., 2006), are shown at low magnifications in Fig. 1. Even at this resolution, however, surface features are clearly evident and well preserved. The particles are fairly uniform in diameter. Measurement of the heights of 124 specimens from different micrographs yielded an average diameter of 83.6 nm with an estimated standard deviation of 5.1 nm. This might represent a slight underestimate of the true size because of some vertical deformation due to cantilever tip pressure. The diameter from EM measurements was 75 nm (Ulbrich et al., 2006).

Fig. 2 shows the particles at higher magnification. The surface is an assembly of lattice domains composed of protein units which form a regular array of rings with large central holes. The center to center distance of the holes, based on 120 measurements, is 8.7 nm. The discontinuities and defects that subdivide the particle surfaces are similar to grain boundaries or mosaic blocks in crystals (Buerger, 1960). The shell thickness, presumably, is the length of one CANC protein, which would be 5 to 6 nm. The prominent, periodic network of protein units initially suggested that the particles might possess the icosahedral symmetry common to most spherical virus capsids. This, however, is unlikely to be the case.

The observed lattice, to the resolution of the AFM images, exhibits at least trigonal symmetry, and possibly hexagonal symmetry. This was concluded as well from earlier electron microscopy studies (Nermut et al., 2002). Plane groups p3 and p6 are the only possibilities for trigonal and hexagonal surface lattices made up of enantiomeric units, hence that of the M-PMV ΔProCANC particles must be one of the two. In the high magnification images of Fig. 3, it can be seen that the lattice rings are composed of six discrete globular protein units of 4 to 5 nm diameter, consistent in size with the CANC protein of Mr=35,000. One protein unit is shared between any two adjacent rings, as indicated in Fig. 4a. Such an arrangement, in which one enantiomeric unit is shared between two rings in this way, is consistent only with plane group symmetry p3 also apparent in Fig. 4a. It further follows that the protein units making up the rings cannot be associated with one another as dimers having $C_2$ symmetry, as that would be inconsistent with the p3 plane group symmetry. They can only be independent monomers, or subunits of $C_3$ trimers.

We have assumed here that the protein units comprising the surface lattice of the M-PMV ΔProCANC particles are enantiomorphic, monomeric protein units. Were they dimers of the fusion protein that had $C_2$ symmetry, then the p3 lattice could, in fact, be p6 and icosahedral symmetry would be possible. This is illustrated in Figs. 4a–c. We feel it wise to exercise caution in this regard. Although there is no evidence at this time that ΔProCANC exists as such a dimer, the possibility cannot be discounted.

An icosahedral shell cannot be constructed from a planar array of subunits having underlying p3 symmetry. An icosahedron is derived from a planar array having hexagonal p6 symmetry. While it is true that facets on a large icosahedron may display local plane group symmetry p3, as for example in the Algal viruses CIV and PBCV-1 (Kuznetsov et al., 2005a; Yan et al., 2000), the facets must ultimately be related by fivefold and twofold axes. No ΔProCANC particles that we examined showed the presence of any pentameric symmetry

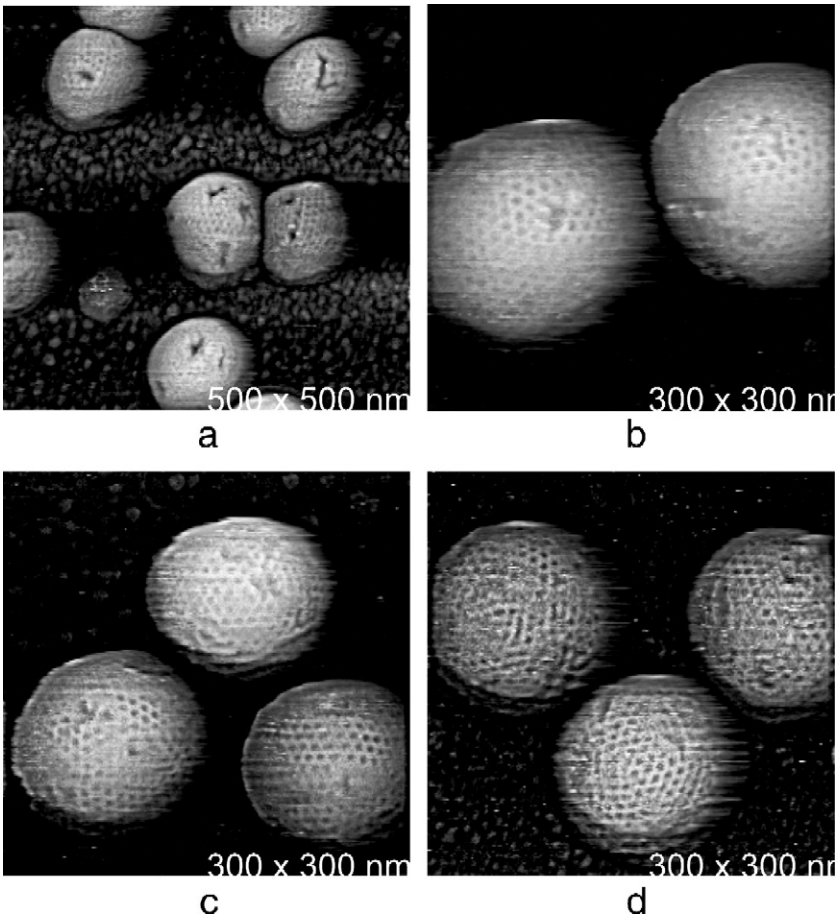


Fig. 1. In (a) through (d) are AFM images at relatively low magnification of spherical particles reassembled *in vitro* from M-PMV ΔProCANC protein produced in bacteria. The particles closely resemble immature virions of M-PMV Gag protein produced by infected mammalian cells. The spherical particles have an average diameter of 83.6 nm as measured by their height above the substrate, and they have a narrow distribution about that average. The substrate also contains a large quantity of macromolecules, principally protein and protein aggregates. The particles, even at this resolution, exhibit two obvious features, an hexagonal network of protein molecules on their surfaces, and the presence of severe defects in the surface lattices.

elements nor of trigonal faces. Such symmetry groupings can, and have been recorded by AFM on other capsids, such as the Ty3 retrotransposons from yeast (Kuznetsov et al., 2005c), on the algal virus PBCV-1 (Kuznetsov et al., 2005a) and a number of other plant and animal viruses (Kuznetsov et al., 2001; Malkin et al., 2004; Plomp et al., 2002). They are not beyond the capabilities of AFM to reveal.

Another prominent feature of the ΔProCANC particle surfaces is the propensity of discontinuities that separate the lattice domains. These are uniformly exhibited by reassembled ΔProCANC particles. We found none during our investigation which failed to exhibit at least one and generally several significant discontinuities or domain boundaries in their surface lattices. Usually the dislocations were obvious. They create deep pits and holes, and in some cases vast fissures which pass to the interior of the particles. It seems most probable that the defects are a natural consequence of the *in vitro* assembly process as they were equally present in samples prepared immediately prior to AFM analysis as well as in old, stored samples.

One approach to determining the fundamental assembly unit of the lattice of the spherical M-PMV particles is to examine some of the smaller defects on their surfaces. Those of limited extent and defined shape are generally a consequence of the loss of one or a small number of building units. This idea was used, for example, to show that the fundamental construction unit of the icosahedral lattice of PBCV-1 Chlorella virus was a symmetrical trimer (Kuznetsov et al., 2005a). We did this for approximately one hundred fifty defects, or scars, on the surfaces of numerous particles. We commonly found some triangular scars, like that in Fig. 5a, indicative of three lattice units, suggesting that a $C_3$ trimer of protein molecules might constitute a building unit. On the other hand, there were many more observations of defects whose shape could be explained by the loss of a single lattice unit. Some of these are shown in Figs. 5b–d.

The two dimensional lattice on the surfaces of the particles is much like a spherical, two dimensional crystal. It may well be that protein units join the lattice and in doing so form threefold symmetric clusters, trimers. Such trimers are a consequence of lattice interactions, however, and may not necessarily preexist in the free state. Trypsin and RNase A, for example, can both be crystallized in trigonal unit cells (Berman et al., 2000), but there is no evidence that either

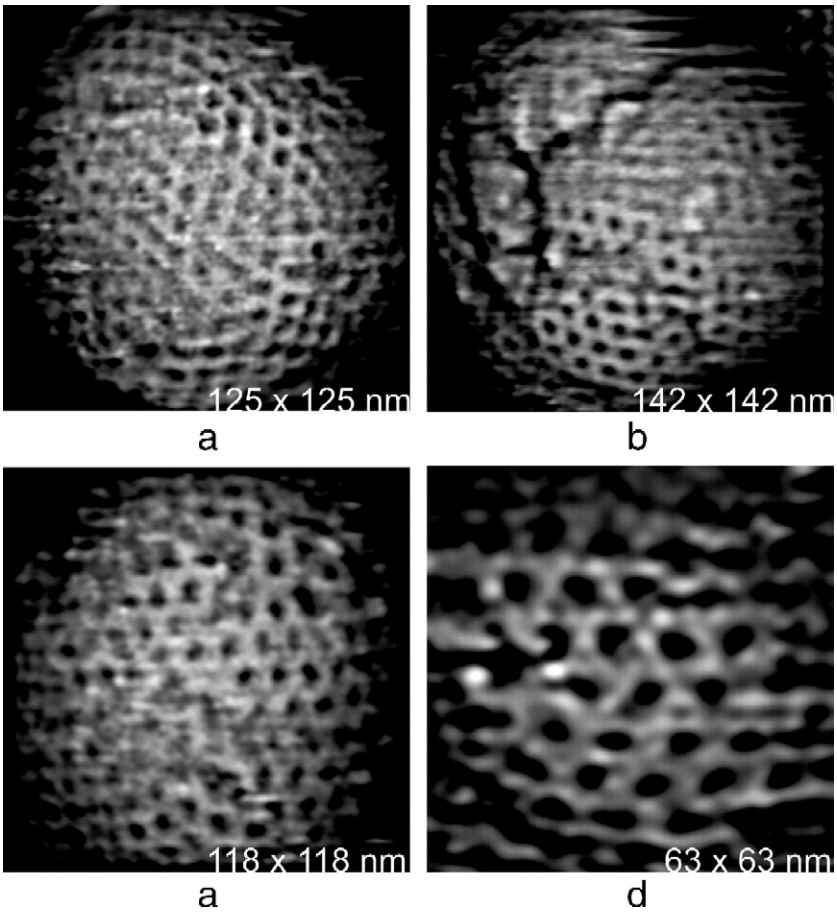


Fig. 2. At moderate magnification, AFM images in (a) through (d) of the M-PMV ΔProCANC protein particles show more clearly the hexagonal network of protein units, and the irregularities, vacancies and discontinuities of the surfaces. The lattices can be seen in many cases to exist as domains, or sectors, that join imperfectly where they meet.

exists as symmetrical trimers in solution. Monomers, dimers and trimers could all separately join a lattice based on p3 symmetry as well, so long as the dimers were not dyad related monomers, but represented two thirds of complete threefold symmetric trimers. This would be consistent with equilibrium of monomers with higher aggregate species in solution, which has been suggested by some crosslinking data (Nermut et al., 2002).

From the measured diameter of 83.6 nm, we can calculate the surface area of the reassembled M-MPV particles to be $4\pi r^2 = 21{,}956$ nm$^2$, and from the center to center distance of the holes, 8.7 nm, the area of the triangles on the particles, $A = 1\ 1/2(8.7\text{ nm})\ (\sqrt{3}/2)\ (8.7\text{ nm}) = 31.28$ nm$^2$. The number of triangles on the particles is, therefore, about 702. If there are 11/2 monomeric protein units per triangle, then the number of fusion proteins making up the particles would be approximately 1050. Previous work based on electron microscopy and using essentially the same calculation resulted in a value of 1200 to 1500 (Ulbrich et al., 2006). This is about half that of previous estimates of the number of protein units in mature HIV-1 capsids (Briggs et al., 2004). If the lattice units were dimers of ΔProCANC, which cannot be completely ruled out, then the number of fusion proteins would be about 2100, but we have no evidence at this time that dimers are the assembly unit.

*Particles reassembled from HIV-1 CANC or ΔProCANC*

Fig. 6 presents low magnification AFM images of tubes formed by HIV-1 CANC protein produced under conditions previously described (Nermut et al., 1998). At low resolution, we could not discriminate between the reassembly products of CANC or ΔProCANC protein from HIV-1. The tube structures appeared the same, at this level of resolution, regardless of the construct. No spherical or polygonal particles of reassembled HIV-1 protein were present in AFM images, though, as noted below, some conical forms were observed.

Evident in Figs. 7a and b is that CANC tubes are in fact left handed helical structures having a high pitch. Although also based on a hexagonal arrangement of protein molecules, the pattern of units comprising the surfaces of the tubes appears substantially different than for the spherical M-PMV particles. Slightly protruding units are seen arranged according to a hexagonal net on the surfaces of the HIV-1 CANC tubes. With the spherical particles of M-PMV, on the other hand, the protein is recessive and large, central holes are prominent. The rows of convex units on the tube surfaces, which have a diameter of 7 to 8 nm, form an angle near 28° with the long axis of a tube.

At high magnification, tubes reassembled from ΔProCANC displayed surfaces with little recognizable structure. Occasion-

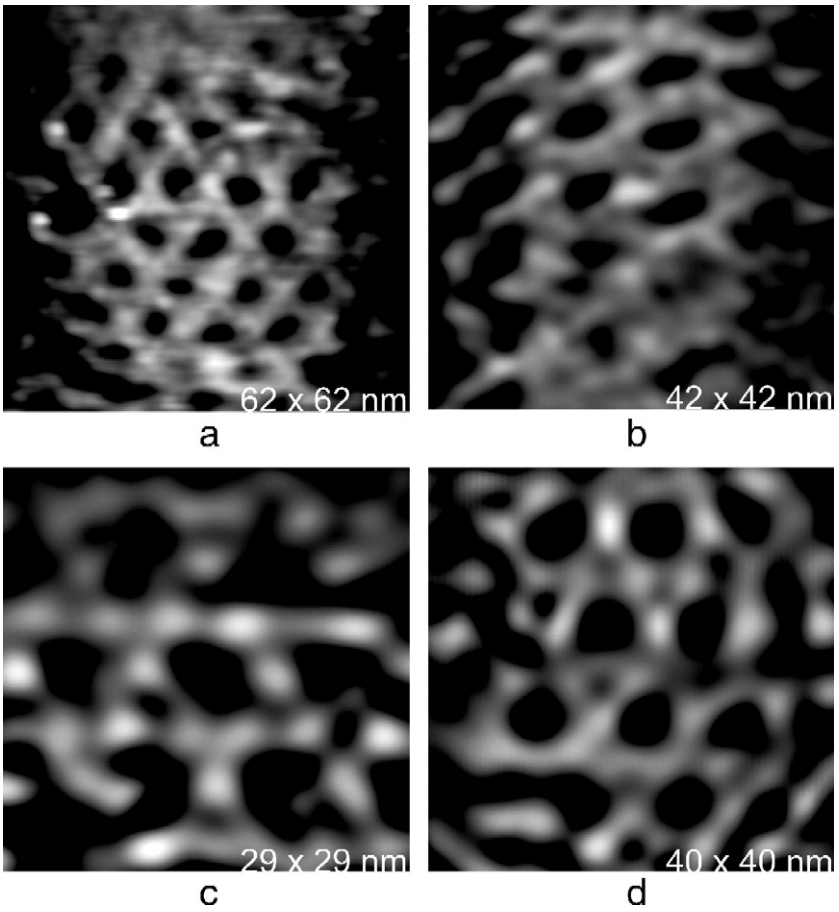


Fig. 3. In (a) through (d) are AFM images of the M-PMV ΔProCANC reassembled particles at high magnification showing some details of the lattice that covers their surfaces. In a number of cases, individual protein units that make up the hexagonal rings can be seen as high features. These images indicate that each protein unit is shared between two hexagonal rings. If the protein units are single copies of the ΔProCANC protein, then the lattice can have only p3 plane group symmetry.

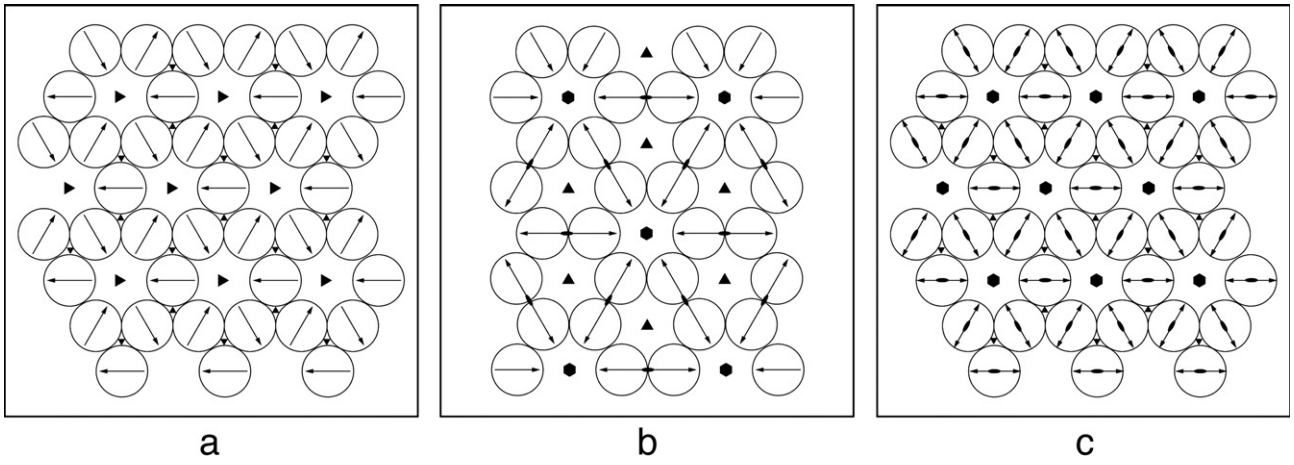


Fig. 4. In (a) is a p3 trigonal lattice composed of asymmetric monomeric proteins. In this lattice, each protein unit is shared equally between two adjacent rings. This lattice appears to be consistent with the distribution of protein units observed in the atomic force micrographs, and with the lattice deduced by electron microscopy for the M-PMV ΔProCANC particles (Nermut et al., 2002). Such a lattice could also be constructed from trimers of the ΔProCANC protein, were the protein to exist in that oligomeric state. In (b) is a p6 trigonal lattice in which no protein units are shared between adjacent rings (hexamers) is distinctly different than the p3 lattice in (a) and could be constructed from HIV-1 CANC protein monomers, dimers or trimers, whatever the case may be. This lattice is consistent with the arrangement of capsomeres on the surfaces of the HIV-1 CANC protein tubes visualized by AFM and is also that previously assigned based on electron microscopy (Ganser et al., 1999). A possibility that must be considered is that the protein units making up the lattice of the M-PMV are not monomers, but $C_2$ dimers. In that case, the lattice in (a) could acquire dyad axes that transform it to p6 symmetry, as shown in (c). This is important because surface lattices having p6 symmetry can form icosahedra, while those with strict p3 plane group symmetry cannot.

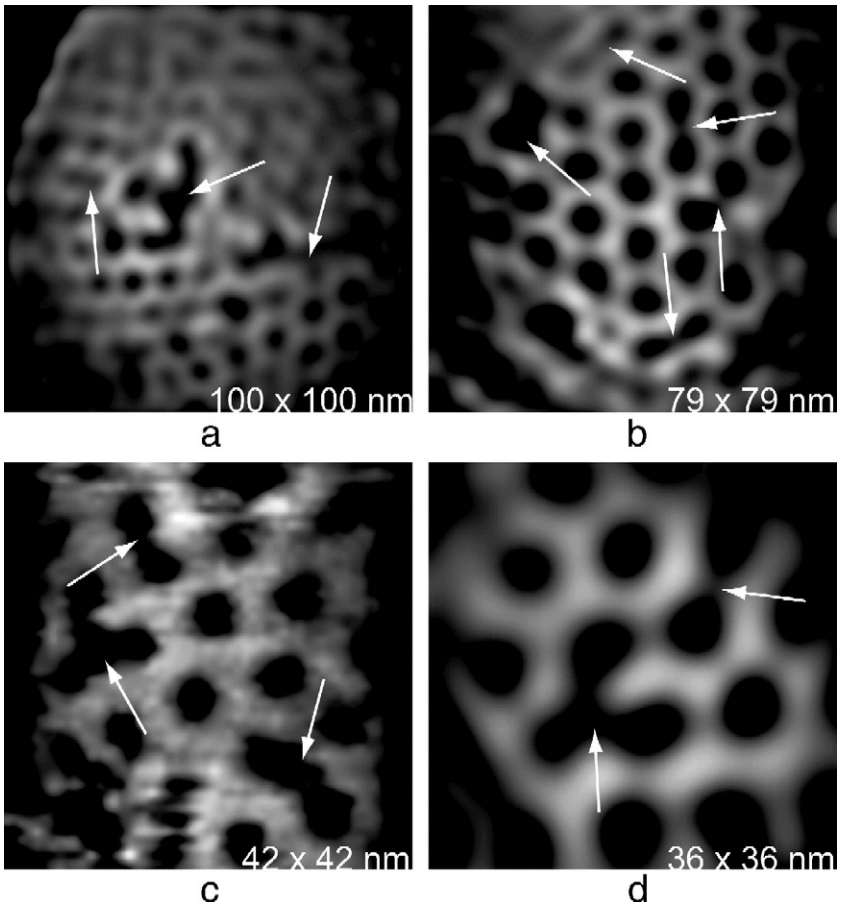


Fig. 5. In (a) through (d) are AFM images of the surfaces of M-PMV ΔProCANC particles showing a variety of defects produced by the loss of one or more protein units. The shapes of the scars can best be explained by the loss of one or more individual protein units, though in some cases the scars could be a consequence of the loss of a trimer.

ally, however, ΔProCANC tubes were seen that did exhibit some degree of order, and this order appeared similar to that seen on the surfaces of the CANC tubes. Although we cannot be certain, we are inclined to believe that both kinds of reassembled tubes are based on the same, or at least similar, underlying ordered structure, but that the surfaces of the ΔProCANC tubes may be more labile and easily disordered.

Tubes of various lengths were observed, but most were of 500 to 600 nm. The diameters were relatively uniform, about 40 nm, based on height measurements. While many tubes appear complete and have a blunt end and a more angular end, others are partially formed and incomplete, ending with rough, irregular termini. Some short tubes, like that in Fig. 8, apparently terminated early after the initiation of assembly, were also seen that were not closed or that remained as almost open sheets. On some of these, we could record the interior surfaces of the tubes, but their appearance was not distinctive.

It was considerably more difficult to obtain high resolution images of the protein lattice forming the reassembled HIV-1 tubes than for the M-PMV particles. In contrast to the M-PMV particles, however, which were characterized by a regular network of prominent holes, the tubes appear to be constructed of distinct protein clusters. These much more resemble conventional capsomeres, protein clusters that protrude slightly from the surfaces. The underlying arrangement of protein clusters on the tubes appears to be based on a hexagonal net in which no protein units are shared between adjacent hexameric clusters. In contrast to the p3 lattice of the M-PMV ΔProCANC particles, the arrangement of capsomeres on the reassembled HIV-1 tubes is most consistent with p6 plane group symmetry.

The distance between neighboring protein clusters is 8.7 nm, the same as that measured between the centers of adjacent rings on the spherical particles of M-PMV. Although we cannot be entirely certain of the details of the protein network making up the reassembled HIV-1 tubes, and in spite of the similarity in distance between lattice units, the underlying arrangement of protein molecules is almost certainly not the same as in the spherical M-PMV particles.

Like the M-PMV particles, the HIV-1 tubes are generally also marked by defects in the surface lattice. The defects, which appear in the reassembled HIV-1 protein tubes, are not the same as those present in the M-PMV spherical particles. Those in M-PMV are discontinuities produced at the intersection of lattice sectors, essentially cracks in the lattice. In the HIV-1 particles, the defects more resemble point defects in crystals, or vacancies, corresponding to the apparent loss of some surface protein

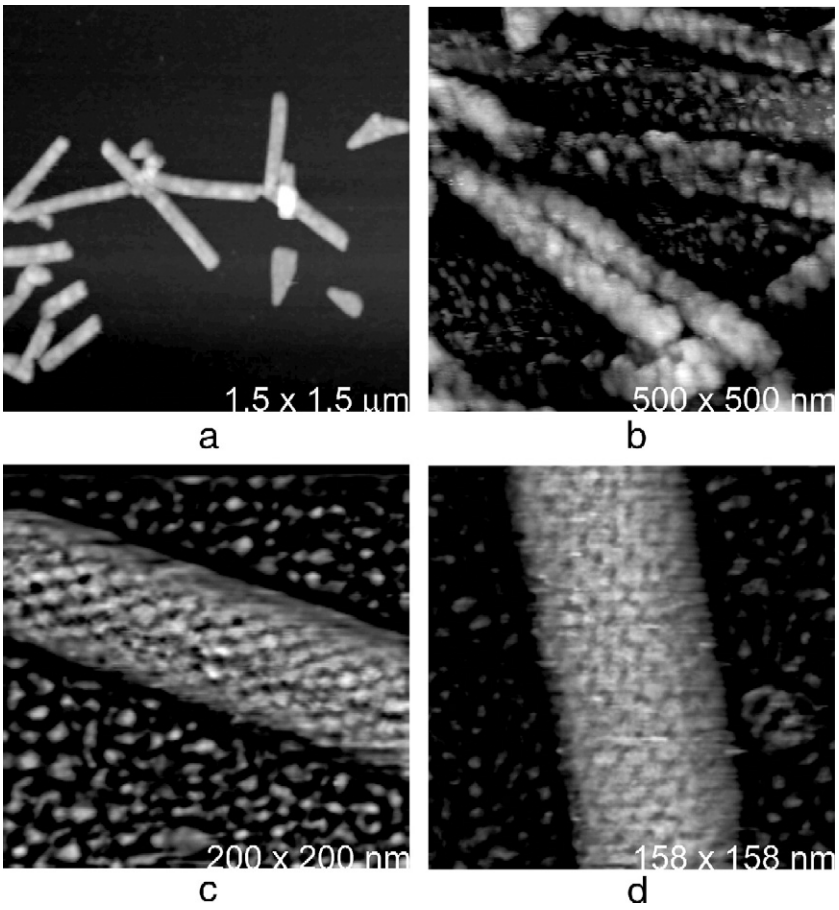


Fig. 6. In (a) is a low magnification AFM image of tubular assemblies of HIV-1 CANC protein, the most common particle design that was encountered. In (b) through (d) tubes are shown at increasingly higher resolution. Though the surface structure is unclear in these images, it does not resemble the surface lattice that covers the M-PMV ΔProCANC particles. The tubes also lack the severe defects and discontinuities that marked the spherical particles.

clusters or lattice units. The defects in the tubes could be due to proteolysis and loss of the exterior domain of the HIV-1 CA protein, which is known to have two domains (Frankel and Young, 1998). In any case, the lack of any distinctive defects, like those seen in the M-PMV particles, is consistent with a fundamental difference in the construction of the two surface lattices.

It may be noteworthy that we observe a large number of reassembled HIV-1 protein tubes which maintain their overall shape, but whose surfaces appear disordered at a detailed level, to such an extent that we can observe no lattice periodicity, only arbitrary aggregates on the tube surfaces. The maintenance of overall architecture, however, suggests that some stable network below the immediate surface, perhaps involving protein associated with a nucleic acid scaffold, may exist. Indeed, strands decorated with protein that we suspect to be RNA were frequently visualized in association with assembling tubes, as in Fig. 8b. This suggests the possibility of a cooperative assembly process involving protein and nucleic acid.

There is an alternate explanation for the maintenance of tube structure even in the absence of an ordered surface lattice. The CA protein of HIV-1 consists of a C-terminal dimerization domain and an N-terminal surface domain. The fundamental structure of the tubes may be a consequence of the ordering of the C-terminal domains into a regular lattice, while the surface N-terminal domains are free to assume more arbitrary dispositions. Because AFM senses only the surface features, AFM images could show a disordered surface structure of N-terminal domains, while an unseen, ordered lattice of C-terminal domains persists. This simple technical point might also explain the different appearances of the surface lattices of the tubes when imaged by AFM and electron microscopy. Being a projection through the entire sample, the latter could reveal an internal, ordered pattern of C-terminal domains, even in the absence of ordered surface domains. AFM, on the other hand, would show the ordered pattern only when the surface domains reflected the pattern of the internal C-terminal domains.

Among the products reassembled from HIV-1 CANC protein were also some conical forms that appear similar to those reported by others (Ganser et al., 1999; Li et al., 2000; Nermut et al., 2002) and resemble as well the mature capsids of HIV-1 (Briggs et al., 2003; Gelderbloom, 1991; Wyma et al., 2000). These may indeed be the same, we cannot be certain. The conical particles seen in Fig. 9 are rather irregular and individual in detailed shape and dimensions. Generally they are 30 to 50 nm in diameter, with lengths of

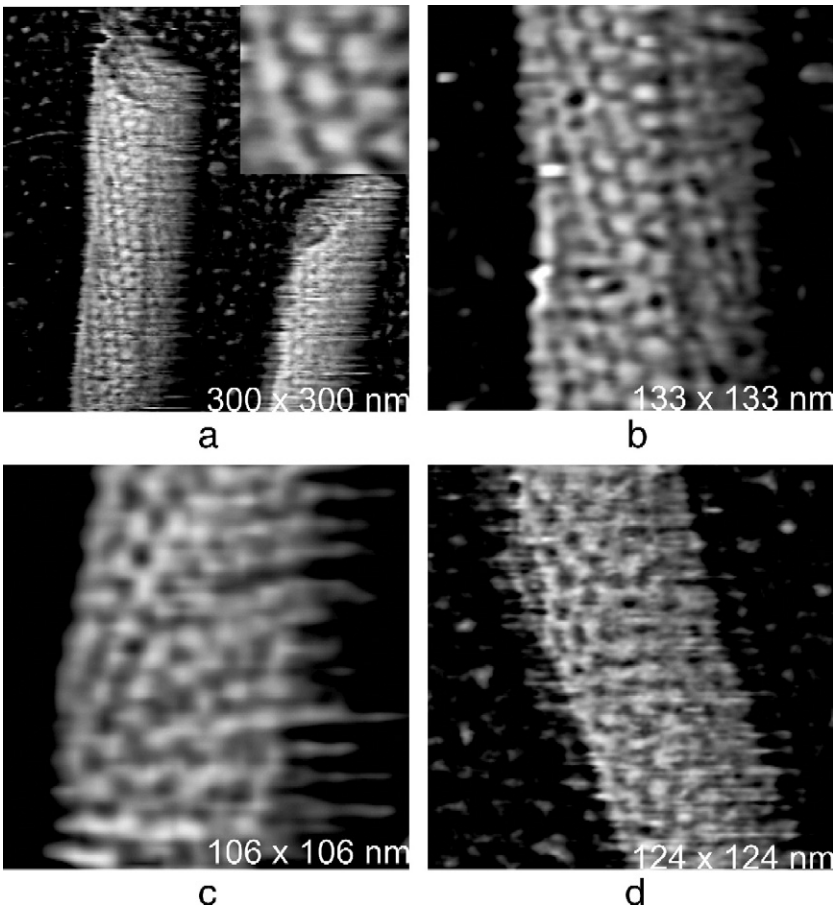


Fig. 7. In higher magnification AFM images in (a) through (d), individual capsomere-like units, presumably protein aggregates, can be seen forming a left handed helical lattice on the surfaces of the HIV-1 CANC tubes. In these structures, there are no hexagonal arrays of rings and holes, but an underlying hexagonal surface lattice made up of slightly protruding, closely packed, capsomeric units. The arrangement seen here is consistent with the lattice based on p6 symmetry that has been proposed previously for the HIV-1 CANC tubular structures.

about 85 to 100 nm. We were unable to obtain clear AFM images of the surfaces of these particles. Some AFM images, however, suggested the presence of an underlying periodic structure that is probably based on the same protein lattice as the HIV-1 CANC tubular structures. This, however, remains to be verified.

The packing of protein units in the lattice of the HIV-1 tubes, which probably reflects that in the mature capsids of HIV-1, is more dense by twice than that of the packing of molecules in the open network of the M-PMV ΔProCANC particles. A spherical HIV-1 capsid of the same diameter as the reassembled M-PMV particles, 83 nm, would, therefore, have twice the number of

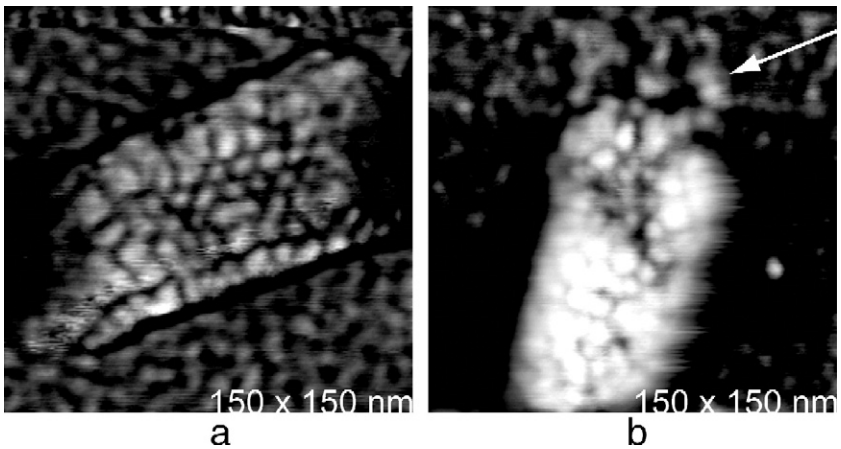


Fig. 8. In (a) is a short segment of HIV-1 CANC tube that forms a curved sheet. The arrangement of protein is similar to what is observed on the tube surface. In (b) is another short segment of a tube, likely terminated during assembly, with one end (top) partially open. Here a linear strand, probably of RNA, can be seen associated with the interior of the tube and extending out onto the substrate. Some protein subunits decorate its length.

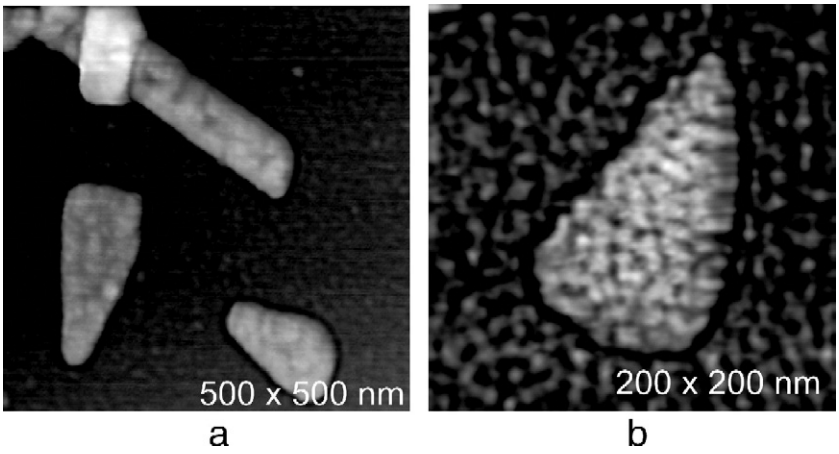


Fig. 9. Occasionally, conical forms, resembling those previously reported for mature HIV-1 capsids (Ganser et al., 1999; Li et al., 2000) and some reassembled particles of HIV-1 CANC protein (Nermut et al., 1998), are seen on the AFM substrate along with tubular structures. These cones are not simply abbreviated tubes as their diameter varies from about 30 nm at the narrow end to about 50 nm at their wide end, neither dimension common to the tubes.

protein molecules, or about 2100. This correlates very well with estimates of 2000 protein molecules in the mature HIV-1 capsid, which were based on other studies (Briggs et al., 2004). By inference, it also supports the estimate of about 1000 monomeric protein molecules in the open lattice covering the surface of the M-PMV particles.

## Discussion

The protein network, according to which the surfaces of the reassembled M-PMV ΔProCANC particles are constructed, was examined in terms of an earlier model proposed by Nermut et al. (2002). In that model, protein trimers were organized according to a network in which one protein subunit was shared between two adjacent hexameric rings of protein. The rings themselves were centered on prominent holes. The center to center distances in that model were 7 nm, a distance derived from electron micrographs. Our AFM images show a center to center distance for the holes of 8.7 nm based on 100 measurements on many particles. Although we can only occasionally see individual protein lattice units in the AFM images, as in Figs. 2 and 3, their arrangement is consistent with the sharing of one lattice unit between adjacent rings. It does not appear to be consistent with the two other alternatives, which are based on the sharing of two or no protein subunits between adjacent rings.

The discrepancy of about 1.7 nm in center to center distance of the holes based on EM and our AFM measurements is a concern. It amounts to a 20% difference in estimations, which is larger than we might have expected. We cannot account for this, except to say that the values by AFM were obtained from more than a hundred measurements on fully hydrated specimens, and the distances were calibrated against a protein crystal of well established lattice parameters.

An icosahedron is constructed from a plane lattice having p6 symmetry by the regular replacement of some hexamers by pentamers. The lattice then becomes quasi symmetric, but the introduction of 12 pentamers imposes curvature and allows it to close into a polygonal shell. The twofold and threefold axes of the p6 plane group persist in the icosahedral particle, and the protein molecules making up the hexamers and pentamers are generally observed to coalesce into discrete, symmetric clusters that we refer to as capsomeres. The capsomeres are usually the most prominent structural units of icosahedral virus capsids (Caspar and Klug, 1962; Horne and Wildy, 1963). An icosahedron cannot be constructed from a two dimensional lattice having plane group symmetry p3, and indeed we find no evidence of icosahedral symmetry in the reassembled M-PMV particles.

The presence of fivefold symmetric, pentameric capsomeres on the surface of a particle is generally taken as the signature feature of an icosahedral particle, which must exhibit twelve in number. Hence, we should occasionally observe a pentamer if we observed no more than one twelfth of a particle. Usually, however, we can clearly see a quarter to a third of the surface of each particle we visualize. We have examined hundreds of particles in completely arbitrary orientations, and still we have never seen a pentamer on the surfaces of the M-PMV ΔPro CANC particles. This exceeds our faith to believe that pentamers are present in the particles we analyzed.

The discontinuities observed to mark the surfaces of the ΔProCANC particles are not simply misfortunes of assembly, but are essential to the overall architecture. It is not possible to spread an exact hexagonal or trigonal net over a spherical surface in a perfect manner, hence the use by viruses of quasi-equivalence and icosahedral symmetry (Caspar and Klug, 1962). In the absence of icosahedral symmetry, as we find here, what is the alternative? It is possible to cover a spherical surface with such nets if one accepts imperfections or discontinuities in the lattice (Bausch et al., 2003; Chamot, 2003). That is, in fact, what we observe to be the case with the M-PMV ΔProCANC particles. The particles are simply imperfect. The surface is a patchwork of ordered domains that allow the particle to assume approximate sphericity using a surface lattice of p3 symmetry.

Similar descriptions of the arrangement of Gag molecules in immature virions of MuLV and HIV-1, based on cryoelectron microscopy, have also been reported (Fuller et al., 1997; Yeager et al., 1998). In those studies, it was observed that sectors of radially directed gag molecules were organized with local hexagonal lattice symmetry, as we see for the M-PMV particles, but that the sectors were misaligned with respect to one another, the same kinds of discontinuities we find. Those investigators also concluded that there was no strict icosahedral symmetry. Whether such symmetry is established upon cleavage of Gag, and maturation, remains unclear.

Exact icosahedral symmetry was found by AFM for retrotransposon particles Ty3 from yeast (Kuznetsov et al., 2005c), and these fell into categories with T numbers of 3, 4 and, predominantly, 7. Such symmetry, up to a triangulation number of $T=9$, was also reported for Ty1 particles based on cryoelectron microscopy (Al-Khayat et al., 1999). This is significant because the Ty1 and Ty3 particles are thought to have structures similar to mature retroviral capsids (Sandmeyer et al., 2002). The work on Ty3 was also based on AFM, so it is unlikely that differences in results could be ascribed to technical points. It must, however, be emphasized that the Ty3 particles were formed naturally in yeast cells, while the M-PMV particles studied here were assembled *in vitro*.

The lattice proposed for the capsids of HIV-1 (Ganser et al., 1999; Nermut et al., 1998) is that shown in Fig. 4b. That lattice, of plane group symmetry p6, as noted above, is consistent with icosahedral particle formation from monomers, dimers or trimers. Indeed, there is evidence that HIV-1 capsids are based on a kind of icosahedral symmetry where the pentamers are not evenly distributed on the particle surfaces. These distorted icosahedra, which have been previously described (Ganser et al., 1999; Li et al., 2000), form conical structures in electron micrographs. M-PMV particles reassembled from monomeric fusion protein could not assume such arrangements. The reassembled particles of M-PMV apparently do not share a common lattice or protein arrangement with native or reassembled HIV-1 capsids. The AFM images show a distinctive difference between the surfaces of the M-PMV and HIV-1 reassembled particles.

Two points are worth noting. First, the reassembled ΔProCANC particles may not, in fact, be identical to immature M-PMV capsids, in spite of their similarity in electron micrographs. It could be argued that true immature capsids of M-PMV have icosahedral symmetry, but it is difficult to see how this could be so since the p3 lattice of the reassembled particles is fundamentally incompatible with icosahedral symmetry. Second, the reassembled particles, which correspond most closely to immature capsids, may be quite different than mature M-PMV capsids. Indeed, a significant, though ill defined, structural transformation is known to occur in retroviruses as a consequence of maturation, and this might involve a general rearrangement of protein units on the surface and the establishment of higher symmetry, one compatible with particle icosahedral symmetry.

Were this the case, it might provide an explanation for the observed differences in the organization of the protein units on the surface of the M-PMV ΔProCANC particles when compared with the reassembled HIV-1 particles. The former may reflect the architecture of the immature retroviral capsid, lacking icosahedral symmetry, while the latter reflects the structure of the mature capsid. The first, it is interesting to note, is based on p3 plane group symmetry, while the latter is based on p6 plane group symmetry. Conversion of plane group p3 to p6 can be affected by the addition of a twofold axis to the p3 symmetry group. That, in turn, could be produced physically by dimerization, during the course of maturation, of CANC monomer pairs into dimers having $C_2$ symmetry. This would not be an implausible event, given that Gag proteins and their domains are known to form dimeric species.

Another alternative exists as well. We noted above that the protein units comprising the surface lattice could conceivably consist of two closely associated M-PMV fusion proteins, rather than one, though we have no evidence for that. If that were so, then expression of latent twofold symmetry and conversion to p6 plane group symmetry could be affected simply through reorientation of a preexisting $C_2$ dimer or a rearrangement of subunits.

There are many examples of spherical viral capsids converting from one architecture to another, and retrovirus capsids perhaps represent another. Bacteriophage HK97, for example, passes through a series of structural states as maturation cleavages in the capsid protein occur (Wikoff et al., 2006), and in other bacteriophages, scaffolding proteins mediate structural transitions (Galisteo and King, 1993). Even in simple icosahedral plant viruses, major rearrangements are known, as for example the conversion of brome mosaic virus, and alfalfa mosaic virus $T=3$ virions into $T=1$ particles upon cleavage of the coat protein (Kumar et al., 1997; Larson et al., 2005).

What we have examined in this study are two reassembled particles that likely exhibit the architectures of immature M-PMV capsids and mature HIV-1 capsids. It is hardly surprising that the two are distinctively different. The question remains whether the differences are due to an inherent difference between the viruses in their structural approach to constructing a capsid or whether the differences are principally a consequence of maturation. If it is the latter, then the two lattices that we visualized here may represent the starting and ending points of the structural transition and thereby significantly constrain its features.

## Materials and methods

### *Preparation of DNA constructs*

Plasmid encoding ΔProCANC of M-PMV was based on pGEMEX-2 bacterial expression vector harboring the whole M-PMV *gag* gene prepared as described previously (Rumlova-Klikova et al., 2000). Plasmids for preparation of HIV-1 ΔProCANC and CA-NC proteins were based on the pET22b expression vector. All cloning steps were carried out by established techniques that are described elsewhere (Sambrook et al., 1989). The cloning strategies and details of the PCR primers can be obtained upon request from the authors. The DNA constructs were verified by DNA sequencing. The

Table 1
AFM measurements of particle dimensions and surface substructures

| M-PMV ΔProCANC spherical particles | HIV CANC tubular particles | HIV conical particles |
|---|---|---|
| (1) Average diameter 83.6 nm, e.s.d. 5.1 nm, from 124 measurements | (1) Average length 500–600 nm | (1) Length, 85 nm to 100 nm |
| (2) Average surface area 21,956 $nm^2$ | (2) Average diameter, 40 nm, e.s.d. 1.5 nm, from 60 measurements | (2) Diameter, 30 nm to 50 nm |
| (3) Average volume 305,927 $nm^3$ | (3) Assuming 600 nm length and 40 nm diameter, (a) surface area 75,398 $nm^2$ (b), volume 753,984 $nm^3$ (c), estimated number of globular units on surface ~1268 | (3) Average cone angle, 30.2° from 8 measurements |
| (4) Center to center distance of holes on surface 8.7 nm e.s.d. 0.4 nm, from 120 measurements | (4) Center to center distance of surface clusters 8.7 nm, e.s.d. 0.5 nm, from 40 measurements | |
| (5) Diameter of globular surface units, 4 nm to 5 nm | (5) Diameter of protein clusters, 7 nm to 8 nm | |
| (6) Estimated shell thickness, 5 nm to 6 nm | (6) Surface lattice symmetry p6 | |
| (7) Number of protein globular units on surface, 1050 | (7) Angle between rows of protein clusters and helix axis, ~28° | |
| (8) Surface lattice symmetry, p3 | (8) Hand of helix, left | |

correct sizes of all expressed proteins were confirmed by SDS-PAGE, and the N-termini were verified by N-terminal sequencing. The vast majority of N-terminal methionine was removed in all cases.

*Expression of M-PMV and HIV-1 genes*

Luria–Bertani (LB) medium containing ampicillin at a final concentration of 100 μg/ml was inoculated with *E. coli* BL21 (DE3) cells carrying the appropriate construct to achieve an optical density $OD_{590}$ ~0.1 and grown at 37 °C. Expression was induced by the addition of isopropyl-β-D-thiogalactopyranoside (IPTG) to a final concentration of 0.4 mM when the cells reached $OD_{590}$ ~0.6–0.8. The cells were harvested 4 h post-induction by low-speed centrifugation and were stored at −20 °C.

*Purification of M-PMV ΔProCANC protein*

The bacterial pellet (from 1 l of cell culture) was resuspended in 30 ml of buffer A (50 mM Tris–HCl, 150 mM NaCl, 1 mM EDTA, pH 8.0) containing lysozyme (1 mg/ml), 0.05% 2-mercaptoethanol, PMSF (100 μg/ml final concentration) and 1.2 ml of Complete (Roche) protease inhibitor mix, and the mixture was stirred at room temperature for 30 min. The cells were sonicated on ice and then treated with sodium deoxycholate (0.1% final concentration) at 4 °C for 30 min. The cell lysate was centrifuged at 10,000×*g* for 10 min at 4 °C. The pellet was resuspended in 10 ml of buffer A containing 0.5% Triton X-100 and 1 M NaCl and then centrifuged at 10,000×*g* for 10 min at 4 °C. The pellet was resuspended in the same volume of buffer A containing 0.5% Triton X-100, 1.5 M NaCl, 0.05% 2-mercaptoethanol and centrifuged again as mentioned above. The supernatants containing ΔProCANC were dialyzed against the buffer Z (50 mM phosphate buffer, pH 7.5, containing 500 mM NaCl) overnight at 4 °C. Dialyzed material was loaded on top of a $Zn^{2+}$-chelating fast flow Sepharose chromatography column (Amersham Pharmacia Biotech) equilibrated in buffer Z. After three washing steps with 50 ml of buffer Z, the bound proteins were eluted with 35 ml of 2 M $NH_4Cl$ in buffer Z. The fractions containing desired protein were combined and dialyzed against buffer B (50 mM Tris–HCl, 100 mM NaCl, 0.01% 2-mercaptoethanol, 1 μM $ZnCl_2$, pH 7.5) overnight at 4 °C. Dialyzed material was then loaded on the phosphocellulose column (Whatman). The purified proteins were eluted using NaCl gradient (100 mM–2 M NaCl in buffer B), and the fractions were analyzed by SDS-PAGE. The fractions containing the required protein were combined, dialyzed overnight against 2 l of buffer C (50 mM phosphate, 500 mM NaCl, 0.01% 2-mercaptoethanol, 1 μM $ZnCl_2$, pH 7.5), concentrated to 1–2 mg/ml by Millipore Centriplus membranes, aliquoted and stored at −20 °C. The protein was determined by SDS-PAGE, and the nucleic acids were determined by spectrophotometry ($A_{260}$ and $A_{280}$) and by the RiboGreen® Assay (Molecular Probes).

*Purification of HIV-1 CANC and ΔProCANC proteins*

We have used the modified method published by Campbell and Vogt (1995) and Ma and Vogt (2004) for purification of HIV-1 proteins. Frozen bacterial pellets (obtained from 1 l of cell culture) were resuspended in 25 ml of buffer D (20 mM Tris–HCl pH 8, 0.5 M NaCl, 10% glycerol, 1 mM EDTA, 1 mM PMSF, 10 mM DTT, 1 mM Triton X-100) on ice. The cells were disrupted by sonication (4×15 s on ice). Insoluble debris and nucleic acids were removed by ultracentrifugation (Beckman TLA 100.3, 65,000 rpm, 3 h, 4 °C) after addition of 0.3% (w/v) polyethyleneimine. The protein was precipitated with 25% saturated ammonium sulfate. After 30 min at 4 °C, the precipitate was collected by centrifugation for 10 min at 12,000×*g* and then resuspended in buffer E (20 mM Tris–HCl pH 8, 10 mM DTT, 1 mM PMSF, 0.1 M NaCl, 50 μM $ZnCl_2$) at 5 ml/l of cell culture. Insoluble material was removed by centrifugation for 4 min at 6000×*g*, and the supernatant was applied on a DEAE-cellulose column. After washing with buffer E, the flow through and washing fractions were pooled and loaded onto a phosphocellulose (Whatman) column. The resin with bound protein was washed with buffer E and then with buffer E containing 0.3 M NaCl. The protein was eluted with buffer E containing 0.5 M NaCl and then with the same buffer containing 1 M NaCl. Proteins were concentrated by ultrafiltration to 1–2 mg/ml, aliquoted and stored at −20 °C. The purity of proteins was confirmed by SDS-PAGE, and the contamination with nucleic acids was assessed by spectrophotometry ($A_{260}$ and $A_{280}$) and by RiboGreen® assay (Molecular Probes).

*In vitro assembly of M-PMV and HIV-1 particles*

An aliquot of 60 μg of purified ΔProCANC or CANC was mixed with MS2 bacteriophage RNA (3569 b) in a ratio of 10:1 (wt/wt). The mixture was dialyzed against buffer containing 50 mM Tris–HCl pH 8, 100 mM NaCl, 1 μM $ZnCl_2$ for 2 h at room temperature. The presence of assembled particles was confirmed by transmission electron microscopy (JEOL JEM-1010) by the methods of negative staining (3% STA, pH 7.2). The mixture was directly used for AFM analysis.

*AFM analysis*

Samples of M-PMV ΔProCANC and HIV-1 fusion protein products formed by *in vitro* assembly were spread on glass cover slips and fixed by *in situ* exposure for 15 min to 5% glutaraldehyde before AFM analysis. Attempts to image unfixed particles failed due to the softness and deformability of the reassembly products. Fixation with glutaraldehyde has been shown in previous studies, to the resolution of the AFM technique, not to perturb the surface structure of viral particles (Kuznetsov et al., 2001, 2002, 2003, 2004, 2005a). The glass cover slip substrate was pretreated with poly-L-lysine to insure adherence of the virus and any other molecules that were present (Table 1).

AFM analysis was carried out using a Nanoscope III multimode instrument (Veeco Instruments, Santa Barbara, CA). The samples were scanned either under buffer or the samples were air-dried after rinsing with water. Reassembled particles, and any associated macromolecules, were scanned at 26 °C using oxide-sharpened silicon nitride tips in a 75 μl fluid cell containing reassembly buffer or in air. For scanning in air, silicon tips were employed. The images were collected in tapping mode (Hansma and Hoh, 1994) with an oscillation frequency of 9.2 kHz in fluid and 300 kHz in air, with a scan frequency of 1 Hz. Procedures were fundamentally the same as described for previous investigations of viruses (Kuznetsov et al., 2001, 2002, 2003; Malkin et al., 2003, 2004) and RNA (Kuznetsov et al., 2005b). In the AFM images presented here, height above substrate is indicated by increasingly lighter color. Thus, points very close to the substrate are dark and those well above the substrate white. Because lateral distances are distorted due to an AFM image being a convolution of the cantilever tip shape with the surface features scanned, quantitative measures of size were based either on heights above the substrate or on center to center distances on particle surfaces. The AFM instrument was calibrated to the small lateral distances by imaging the 111 face of a thaumatin protein crystal and using the known lattice spacings (Ko et al., 1994; Kuznetsov et al., 1999) as standard.

## Acknowledgments

This work was supported by the National Institutes of Health (AM) GM58868 and the Czech Ministry of Education Research Project Grants 1M6837805002NR8797-4/2006 and MSM 6046137305 and NR8797-4/2006 from the Czech Ministry of Health.

## References

Al-Khayat, H.A., Bhella, D., Kenney, J.M., Roth, J.F., Kingsman, A.J., Martin-Rendon, E., Saibil, H.R., 1999. Yeast Ty retrotransposons assemble into virus-like particles whose T-numbers depend on the C-terminal length of the capsid protein. J. Mol. Biol. 292 (1), 65–73.

Bausch, A.R., Bowick, M.J., Cacciuto, A., Dinsmore, A.D., Hsu, M.F., Nelson, D.R., Nikolaides, M.G., Travesset, A., Weitz, D.A., 2003. Grain boundary scars and spherical crystallography. Science 299, 1716–1718.

Berman, H.M., Westbrook, J., Feng, Z., Gilliland, G., Bhat, T.N., Weissig, H., Shindyalov, I.N., Bourne, P.E., 2000. The protein data bank. Nucleic Acids Res. 28, 235–242.

Briggs, J.A.G., Wilk, T., Welker, R., Krausslich, H.-G., Fuller, S.D., 2003. Structural organization of authentic, mature HIV-1 virions and cores. EMBO J. 22 (7), 1707–1715.

Briggs, J.A., Simon, M.N., Gross, I., Krausslich, H.G., Fuller, S.D., Vogt, V.M., Johnson, M.C., 2004. The stoichiometry of Gag protein in HIV-1. Nat. Struct. Mol. Biol. 11 (7), 672–675.

Buerger, M.J., 1960. Crystal Structure Analysis. John Wiley and Sons, New York, NY.

Campbell, S., Vogt, V.M., 1995. Self-assembly in vitro of purified CA-NC proteins from Rous sarcoma virus and human immunodeficiency virus type 1. J. Virol. 69, 6487–6497.

Caspar, D.L.D., Klug, A., 1962. Cold Spring Harbor Symp. Quant. Biol.

Chamot, J., 2003. Researchers solve 100-year old puzzle of how layer of particles coats the surface of a sphere. Science 299.

Frankel, A.D., Young, J.A.T., 1998. HIV-1: fifteen proteins and an RNA. Annu. Rev. Biochem. (67), 1–25.

Fuller, S.D., Wilk, T., Gown, B.E., Krausslich, H.-G., Vogt, V.M., 1997. Cryo-electron microscopy reveals ordered domains in the immature HIV-1 particle. Curr. Biol. 7, 729–738.

Galisteo, M.L., King, J., 1993. Conformational transformations in the protein lattice of phage P22 procapsids. Biophys. J. 65 (1), 227–235.

Ganser, B.K., Li, S., Klishko, V.Y., Finch, J.T., Sundquist, W.I., 1999. Assembly and analysis of conical models for the HIV-1 core. Science 283, 80–82.

Ganser, B.K., Cheng, A., Sundquist, W.I., Yeager, M., 2003. Three-dimensional structure of the M-MuLV CA protein on a lipid monolayer: a general model for retroviral capsid assembly. EMBO J. 22 (12), 2886–2892.

Gelderbloom, H.R., 1991. Assembly and morphology of HIV: potential effect of structure on viral function. AIDS 5, 617–637.

Hansma, H.G., Hoh, J.H., 1994. Biomolecular imaging with the atomic force microscope. Annu. Rev. Biophys. Biomol. Struct. 23, 115–139.

Horne, R.W., Wildy, P., 1963. Virus structure revealed by negative staining. Adv. Virus Res. 10, 101–170.

Klikova, M., Rhee, S.S., Hunter, E., Ruml, T., 1995. Efficient in vivo and in vitro assembly of retroviral capsids from Gag precursor proteins expressed in bacteria. J. Virol. 69 (2), 1093–1098.

Ko, T.P., Day, J., Greenwood, A., McPherson, A., 1994. Structures of three crystal forms of the sweet protein thaumatin. Acta Crystallogr., D Biol. Crystallogr. 50 (Pt 6), 813–825.

Kumar, A., Reddy, V.S., Yusibov, V., Chipman, P.R., Hata, Y., Fita, I., Fukuyama, K., Rossmann, M.G., Loesch-Fries, L.S., Baker, T.S., Johnson, J.E., 1997. The structure of alfalfa mosaic virus capsid protein assembled as a $T=1$ icosahedral particle at 4.0-A resolution. J. Virol. 71 (10), 7911–7916.

Kuznetsov, Y.G., Konnert, J., Malkin, A.J., McPherson, A., 1999. The advancement and structure of growth steps on thaumatin crystals visualized by atomic force microscopy at molecular resolution. Surf. Sci. 440, 69–80.

Kuznetsov, Y.G., Malkin, A.J., Lucas, R.W., Plomp, M., McPherson, A., 2001. Imaging of viruses by atomic force microscopy. J. Gen. Virol. 82 (Pt 9), 2025–2034.

Kuznetsov, Y.G., Datta, S., Kothari, N.H., Greenwood, A., Fan, H., McPherson, A., 2002. Atomic force microscopy investigation of fibroblasts infected with wild-type and mutant murine leukemia virus (MuLV). Biophys. J. 83 (6), 3665–3674.

Kuznetsov, Y.G., Victoria, J.G., Robinson, W.E.J., McPherson, A., 2003. Atomic force microscopy investigation of HIV and HIV-infected lymphocytes. J. Virol. 77 (22), 11896–11909.

Kuznetsov, Y.G., Victoria, J., Low, G.A., Robinson, W.E.J., Fan, H., McPherson, A., 2004. AFM imaging of retroviruses HIV and MuLV. Scanning 26, 209–216.

Kuznetsov, Y.G., Gurnon, J.R., Van Etten, J.L., McPherson, A., 2005a. Atomic force microscopy investigation of a chlorella virus, PBCV-1. J. Struct. Biol. 149 (3), 256–263.

Kuznetsov, Y.G., Daijogo, S., Zhou, J., Semler, B.L., McPherson, A., 2005b. Atomic force microscopy analysis of icosahedral virus RNA. J. Mol. Biol. 347 (1), 41–52.

Kuznetsov, Y.G., Zhang, M., Menees, T.M., McPherson, A., Sandmeyer, S., 2005c. Investigation by atomic force microscopy of the structure of Ty3 retrotransposon particles. J. Virol. 79 (13), 8032–8045.

Larson, S.B., Lucas, R.W., McPherson, A., 2005. Crystallographic structure of the $T=1$ particle of brome mosaic virus. J. Mol. Biol. 346 (3), 815–831.

Li, S., Hill, C.P., Sundquist, W.I., Finch, J.T., 2000. Image reconstructions of helical assemblies of the HIV-1 CA protein. Nature 407, 409–413.

Ma, Y.M., Vogt, V.M., 2004. Nucleic acid binding-induced Gag dimerization in the assembly of Rous sarcoma virus particles in vitro. J. Virol. 78, 52–60.

Malkin, A.J., McPherson, A., Gershon, P.D., 2003. Structure of intracellular mature vaccinia virus visualized by in situ AFM. J. Viol. 77 (11), 6332–6340.

Malkin, A.J., Plomp, M., McPherson, A., 2004. Unraveling the architecture of viruses by high-resolution atomic force microscopy. In: Lieberman, P.M. (Ed.), Virus Structure and Imaging, DNA Viruses, Methods and Protocols. Humana Press, Totowa, NJ, pp. 85–108.

Mayo, K., Vana, M.L., McDermott, J., Huseby, D., Leis, J., Barklis, E., 2002. Analysis of Rous sarcoma virus capsid protein variants assembled on lipid monolayers. J. Mol. Biol. 316, 667–678.

Mayo, K., Huseby, D., McDermott, J., Arvidson, B., Finlay, L., Barklis, E., 2003. Retrovirus capsid protein assembly arrangements. J. Mol. Biol. 325, 225–237.

McDermott, J., Mayo, K., Barklis, E., 2000. Three-dimensional organization of retroviral capsid proteins on a lipid monolayer. J. Mol. Biol. 302, 121–133.

Nermut, M.V., Hockley, D.J., Bron, P., Thomas, D., Zhang, W.H., Jones, I.M., 1998. Further evidence for hexagonal organization of HIV gag protein in prebudding assemblies and immature virus-like particles. J. Struct. Biol. 123 (2), 143–149.

Nermut, M.V., Bron, P., Thomas, D., Rumlova, M., Ruml, T., Hunter, E., 2002. Molecular organization of Mason–Pfizer monkey virus capsids assembled from Gag polyprotein in *Escherichia coli*. J. Virol. 76 (9), 4321–4330.

Plomp, M., Rice, M.K., Wagner, E.K., McPherson, A., Malkin, A.J., 2002. Rapid visualization at high resolution of pathogens by atomic force microscopy: structural studies of herpes simplex virus-1. Am. J. Pathol. 160 (6), 1959–1966.

Rumlova-Klikova, M., Hunter, E., Nermut, M.V., Pichova, I., Ruml, T., 2000. Analysis of Mason–Pfizer monkey virus Gag domains required for capsid assembly in bacteria: role of the N-terminal proline residue of CA in directing particle shape. J. Virol. 74 (18), 8452–8459.

Sambrook, J., Fritsch, E.F., Maniatis, T., 1989. A Laboratory Manual. Molecular Cloning, 2nd ed. Cold Spring Harbor Laboratory Press, Cold Spring Harbor, NY.

Sandmeyer, S.B., Aye, M., Menees, T.M., 2002. Ty3: a position-specific gypseylike element in *Saccharomyces cerevisiae*. In: Craig, N.L., Craigie, R., Gellert, M., Lambowitz, A.M. (Eds.), Mobile DNA. ASM Press, Washington, DC.

Ulbrich, P., Haubova, S., Nermut, M.V., Hunter, E., Rumlova, M., Ruml, T., 2006. Distinct roles for nucleic acid in in vitro assembly of purified Mason–Pfizer monkey virus CANC proteins. J. Virol. 80 (14), 7089–7099.

Wikoff, W.R., Conway, J.F., Tang, J., Lee, K.K., Gan, L., Cheng, N., Duda, R.L., Hendrix, R.W., Steven, A.C., Johnson, J.E., 2006. Time-resolved molecular dynamics of bacteriophage HK97 capsid maturation interpreted by electron cryo-microscopy and X-ray crystallography. J. Struct. Biol. 153 (3), 300–306.

Wyma, D.J., Kotov, A., Aiken, C., 2000. Evidence for a stable interaction of gp41 with Pr55 Gag in immature human immunodeficiency virus type 1 particles. J. Virol. 74 (20), 9381–9387.

Yan, X., Olson, N.H., Van Etten, J.L., Bergoin, M., Rossmann, M.G., Baker, T.S., 2000. Structure and assembly of large lipid-containing dsDNA viruses. Nat. Struct. Biol. 7 (2), 101–103.

Yeager, M., Wilson-Kubalek, E.M., Weiner, S.G., Brown, P.O., Rein, A., 1998. Supramolecular organization of immature and mature murine leukemia virus revealed by electron cryo-microscopy: implications for retroviral assembly mechanisms. Proc. Natl. Acad. Sci. U. S. A. 95, 7299–7304.